International Journal of Greenhouse Gas Control, Vol. 70, March 2018, pp. 45-56
DOI:10.1016/j.ijggc.2018.01.010

Techno-economic evaluation of the 2-amino-2-methyl-1-propanol (AMP) process for CO_2 capture from natural gas combined cycle power plant

*Ebuwa Osagie, Chechet Biliyok, Giuseppina Di Lorenzo, Dawid P. Hanak, Vasilije Manovic**

Combustion and CCS Centre, Cranfield University,

Bedford, Bedfordshire, MK43 0AL, UK

**Corresponding author: Vasilije Manovic*

Email: v.manovic@cranfield.ac.uk, *Phone: +44(0)123475 4649*

Abstract

It is widely accepted that emissions of CO_2, which is a major greenhouse gas, are the primary cause of climate change. This has led to the development of carbon capture and storage (CCS) technologies in which CO_2 is captured from large-scale point sources such as power plants. However, retrofits of carbon capture plants result in high efficiency penalties, which have been reported to fall in the range of 7–12% points in the case of post-combustion capture from natural gas-fired power plants. Therefore, a reduction of these efficiency losses is a high priority in order to deploy CCS at a large scale. At the moment, chemical solvent scrubbing using amines, such as monoethanolamine (MEA), is considered as the most mature option for CO_2 capture from fossil fuel-fired power plants. However, due to high heat requirements for solvent regeneration, and thus high associated efficiency penalties, the use of alternative solvents has been considered to reduce the energy demand. In this study, a techno-economic assessment of the post-combustion CO_2 capture process using 2-amino-2-methyl-1-propanol (AMP) for decarbonisation of a natural gas combined cycle (NGCC) power plant was performed. The thermodynamic assessment revealed that the AMP-based process resulted in 25.6% lower reboiler duty compared to that of the MEA-based process. This was primarily because the AMP solvent can be regenerated at a higher temperature (140°C) and pressure (3.5 bar) compared to that of MEA (120°C and 1.8 bar). Furthermore, the efficiency penalty due to the retrofit of the AMP-based process with the natural gas combined cycle power plant was estimated to be 7.1% points, compared to 9.1% points in the case of integration with the MEA-based process. Regardless of the superior thermodynamic performance, the economic performance of the AMP-based process was shown to be better than that of the MEA-based process only for make-up rates below 0.03%. Therefore, use of AMP as a solvent in chemical solvent scrubbing may not be the most feasible option from the economic standpoint, even though it can significantly reduce the efficiency penalty associated with CO_2 capture from NGCCs.

Keywords: Natural gas combined cycle, AMP, MEA, Post-combustion capture, Techno-economic analysis, Modelling and simulation, Operating conditions

Nomenclature

AMP	2-amino-2-methyl-1-propanol
CCS	Carbon Capture and Storage
CCU	CO_2 Compression Unit
DCC	Direct Contact Cooler
DEA	Diethanolamine
DGA	Diglycolamine
DOE	Department of Energy
HP	High Pressure
HRSG	Heat Recovery Steam Generator
IEA	International Energy Agency
IP	Intermediate Pressure
LCOE	Levelised Cost of Electricity
LHV	Lower Heating Value
LP	Low Pressure
MDEA	Methyldiethanolamine
MEA	Monoethanolamine
NETL	National Energy Technology Lab
NGCC	Natural Gas Combined Cycle
O&M	Operation and Maintenance
PCC	Post-combustion Capture
PZ	Piperazine
TEA	Triethanolamine

Notation

C_o	Capacity factor (-)
D	Diameter (m)
F_p	Packing factor (m^{-1})
G	Gas flowrate (kg/s)
L	Liquid flowrate (kg/s)
U_s	Superficial velocity (m/s)
V	Kinematic viscosity (m^2/s)
X	Flow parameter (-)
ρ_g	Density of the gas (kg/m^3)
ρ_L	Density of liquid (kg/m^3)

1. Introduction

The increasing concentrations of greenhouse gases in the atmosphere, primarily CO_2, are regarded as being responsible for changes in climate. As identified by the International Energy Agency (IEA), carbon capture and storage (CCS) is one of the viable mitigation strategies that will help meet the emission reduction targets by 2050 [1]. However, the costs associated with commercial-scale capture plants are a major challenge for implementation of CCS [2].

Chemical absorption processes employing primary alkanolamines, such as methanolamine (MEA), have already been used in several industrial processes for over 50 years [3,4]. The absorption process is based on the exothermic reaction of CO_2 from flue gas and amines in the solvent via a zwitterion mechanism to form carbamates. Therefore, heat is required for solvent regeneration [4], and the development and use of amine-based solvents with lower energy requirements for regeneration, along with enhanced reaction kinetics and mass transfer properties, is a major research priority. The heat required for the solvent regeneration is typically provided by means of steam extraction from the power cycle [5]. However, it results in lower thermal efficiency and lower power output, and finally, in economic penalties. Therefore, substitute solvents are expected to enable reducing the amount of steam taken from the power cycle required for their regeneration.

Solvents that can potentially substitute conventionally considered MEA include diethanolamine (DEA), triethanolamine (TEA), n-methyl diethanolamine (MDEA), 2-amino-methyl-1-propanol (AMP), diglycolamine (DGA), piperazine (PZ) and ammonia. MEA, DEA, AMP, and MDEA are the major alkanolamine absorbents in industrial processes [6]. MEA is the default solvent choice because of its reaction kinetics when absorbing CO_2 [7], and it is relatively low in cost. DEA (secondary amine) is less reactive than MEA and undergoes a number of irreversible reactions with CO_2, forming products that are corrosive [8]. MDEA (tertiary amine) is also characterised by a lower CO_2 absorption rate than MEA [9–11]. The mechanism of CO_2 absorption is different when compared to primary and secondary amines, i.e., there is no direct reaction with CO_2 and the N−H bond needed to form the carbamate ion is not present [9].

Similarly to MEA, AMP is a primary amine, sterically hindered, and it was first proposed by Satori and Savage [10] as a substitute for MEA. It has been noted that, due to the steric effects, the stability of the formed carbamate is reduced resulting in a lower heat of reaction compared to that in the case of MEA [12]. Also, AMP forms bicarbonates and theoretical loading capacity is 1 mol CO_2/mol AMP, which is double that of MEA [13]. Furthermore, AMP is more chemically and thermally stable with degradation rates close to half those observed for MEA. For these reasons, saturated AMP solvent can be regenerated at higher temperatures, enabling stripper operation under elevated pressure (up to 30% higher than that of MEA). This, in turn, reduces the CO_2 compression ratio, efficiency penalties, capital costs, and hence favours the economics of AMP-based CO_2 scrubbing. Also, due to the higher regeneration temperature, which can be up to 140°C, 20°C higher compared to MEA, the solvent viscosity is reduced [14]. In addition, AMP is less corrosive enabling the use of higher concentrations, leading to a greater absorption capacity [15,16]. However, Gabrielsen et al. [13] highlighted difficulties in using 40%$_{wt}$ AMP due to the formation of wax-like white solid when the absorbent is saturated with CO_2. Also, the absorption rate of AMP is lower than that of MEA, which appears to be the major drawback of AMP solvent [13,15,17].

A number of modelling studies aimed to analyse CO_2 absorption in packed columns using AMP [13,18–22], but very few studies have considered the integration of the power plant with the capture plant. Van der Spek et al. [23] employed the rate-based approach to post-combustion capture (PCC) modelling and compared the thermodynamic performance of a coal-fired power plant retrofitted with a PCC plant using AMP/PZ and MEA solvents, considering the same operating conditions. Their results showed that using AMP/PZ resulted in better performance, which was characterised by a 1%-point higher net efficiency. Sanchez et al. [24] analysed the thermodynamic performance of natural gas combined cycle (NGCC) and advanced supercritical pulverised coal power plants retrofitted with PCC plants using MEA and CESAR-1 (AMP+PZ), considering the same operating conditions for both solvents. An equilibrium-based capture model was used and their results showed better performance of the retrofitted system in the case of AMP/PZ. The techno-economic analysis of the MEA and AMP/PZ processes, also considering the same operating conditions for both solvents, has only been presented by Manzolini et al. [25], and showed 1% lower cost of electricity in the case of the AMP/PZ-based system. However, no study has yet evaluated the

techno-economic performance of the PCC retrofit using only AMP solvent with the stripper operating at elevated temperature and pressure.

Therefore, the aim of this work is to evaluate the techno-economic feasibility of the AMP-based process for CO_2 capture at a commercial scale, considering higher stripper pressure, higher solvent concentration, and higher loading. An AMP pilot-scale capture plant process model is scaled up to commercial scale, using Aspen Plus® V8.4. The best mass transfer correlation set for the AMP-based process among three options is identified and near-optimal operating conditions were determined by a sensitivity analysis. Furthermore, the AMP-based process model is retrofitted into an NGCC power plant model with a key feature of implementation of the Stodola's ellipse to account for the pressure drop due to steam extraction in order to provide better efficiency estimates. Finally, the economic performance of the retrofitted system is evaluated, and compared to that based on MEA.

2. Capture plant modelling

2.1. Model description

.The PCC plant consists of two columns (absorber and stripper), a cross-heat exchanger represented by two heaters, a cooler and two pumps, connected in a closed cycle to achieve good prediction of the performance of the process [26]. Rich AMP leaving the bottom of the absorber is pumped to the cross-heat exchanger, and exchanges heat with the lean solvent leaving the reboiler before entering the stripper. The lean solvent from the stripper is then pumped and further cooled down before it is fed to the absorber. More details on the AMP-based capture plant and design of absorber and stripper columns can be found in the literature [19,27].

2.2.Model validation

The AMP-based process model is validated with pilot plant data reported by Gabrielsen et al. [13], for which the main design parameters are presented in Table 1. Three cases of experimental data (R4, R7, and R11) obtained for process parameters presented in Table 2 are chosen for model validation. These were selected from 11 experimental tests performed by Gabrielsen et al. [13], due to their different operating conditions, and the accuracy of mass balances.

Table 1. Design data of the pilot plant [13]

	Absorber	Stripper
Diameter (m)	0.15	0.10
Packing height (m)	4.36	3.89
Packing	Sulzer Mellapak 250Y	Sulzer Mellapak 250Y
Type of packing	Structured	Structured

Table 2. Input parameters for validation of absorber model [13]

	Input Parameters			
Case	Lean loading (mol/mol)	AMP concentration (mol/L)	Gas flowrate (m^3/h)	Solvent flowrate (L/h)
4	0.118	2.89	119	3.0
7	0.170	2.89	118	3.0
11	0.284	2.89	122	6.0

2.2.1. Absorber model validation

It can be seen in Table 3 that the best agreement between experimental and simulation results using the three different sets of mass transfer correlations is in the case of the Billet and Schultes correlation [28], with discrepancies for the capture level and rich loading lower than 7%. The largest difference observed in the case of the other two sets of mass transfer correlations is almost 20% for the capture level (Case 4), implying that these correlations may have limited application for the AMP-based process.

Table 3. Comparison of model predictions with experimental data for the absorber

	Rich loading (mol/mol)			Capture level (%)		
	Bravo and Rocha correlations [29]					
Case	Experiment	Model	Difference (%)	Experiment	Model	Difference (%)
4	0.379	0.403	6.0	29.85	24.79	17.0
7	0.459	0.412	10.5	24.15	21.44	11.2
11	0.400	0.399	0.2	22.00	19.40	11.8
	Billet and Schultes correlations [28]					
4	0.379	0.404	6.1	29.85	28.81	3.5
7	0.459	0.455	0.4	24.15	25.37	4.8
11	0.400	0.415	3.6	22.00	21.97	0.1
	Bravo et al. correlations [30]					
4	0.379	0.368	2.9	29.85	24.05	19.4
7	0.459	0.399	13.0	24.15	20.94	13.3
11	0.400	0.391	2.2	22.00	19.35	12.0

Fig. 1 presents the comparison of temperature profiles in the absorber showing good agreement between the experimental data and simulations for all three sets of mass transfer correlations. Specifically, the trend and the temperature bulge in the column are properly predicted. This bulge is dependent on the L/G ratio and shows the location in the column where CO_2 absorption and heat release are the most intensive [31]. Some discrepancies between experiments and model remain, and they are more pronounced with increasing L/G ratio for all three sets of the mass transfer correlations. In addition, the model underestimates the temperatures in the absorber, which implies that the model slightly underestimates the capture levels in the absorber, which is in agreement with the results presented in Table 3. In conclusion, the Billet and Schultes correlations [28] enable proper model predictions for the capture level, rich loading, and absorber temperature profiles that are very close to the pilot plant data and, therefore, can be used in a scaled-up and integrated process model.

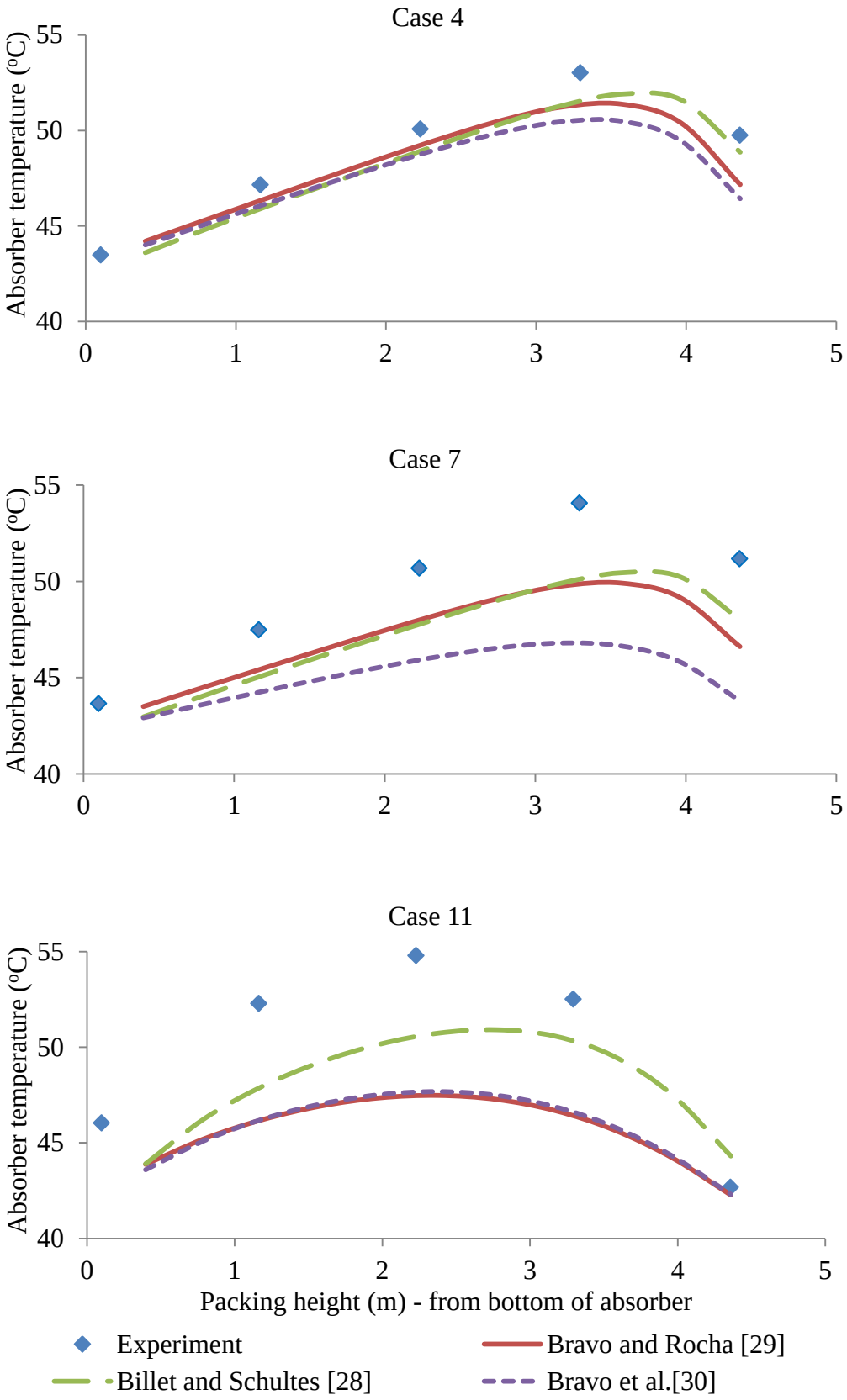

Fig. 1. Liquid phase temperature profiles in the absorber

2.2.2 Stripper model validation

Input parameters for validation of the stripper model are presented in Table 4 [13]. It can be seen in Table 5 that the model predictions closely fit the pilot plant data for all three sets of mass transfer correlations, with some better agreement in the case of the Bravo and Rocha [29] and Bravo et al. [30] correlations. Fig. 2 shows the temperature profiles in the stripper for the three cases, which are very similar for all three sets of mass transfer correlations and fit the pilot plant data. Both pilot plant data and simulations show similar L-shape profiles expected for a stripper. This confirms that the model can be scaled up and integrated, and the Bravo and Rocha correlations [29] are selected due to the closest predictions.

Table 4. Input parameters for validation of stripper model [13]

Case	Rich loading (mol/mol)	Reboiler duty (kW)	Condenser temperature (°C)
4	0.379	7.6	16
7	0.459	7.6	19
11	0.400	7.7	14

Table 5. Comparison of model predictions with experimental data for the stripper

	Lean out (mol/mol)			Reboiler temperature (°C)		
			Bravo and Rocha correlations [29]			
Case	Experiment	Model	Difference (%)	Experiment	Model	Difference (%)
4	0.118	0.120	1.7	117	118	0.9
7	0.170	0.181	6.1	112	115	2.7
11	0.284	0.278	2.1	107	112	4.7
			Billet and Schultes correlations [28]			
4	0.118	0.115	2.6	117	118	0.9
7	0.170	0.182	6.6	112	115	2.7
11	0.284	0.278	2.1	107	112	4.7
			Bravo et al. correlations [30]			
4	0.118	0.121	2.5	117	118	0.9
7	0.170	0.182	6.6	112	115	2.7
11	0.284	0.278	2.1	107	112	4.7

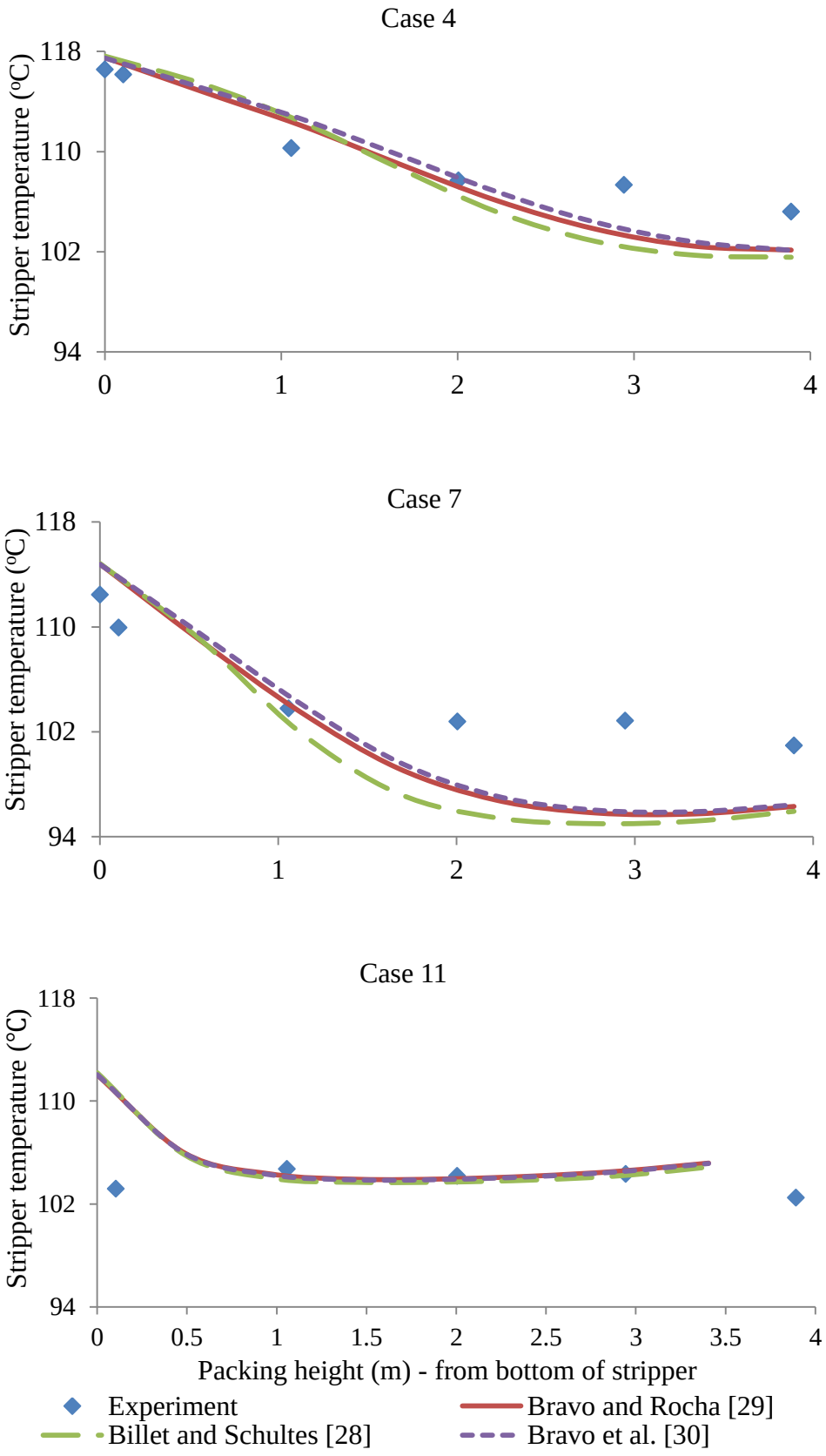

Fig. 2. Liquid phase temperature profiles in the stripper

3. Scale-up of the capture plant model

3.1. Considerations

AMP has a lower CO_2 absorption rate than MEA, which is a major drawback of AMP solvent compared to MEA. The absorption rate can be enhanced by increasing the surface area of packing, increasing the absorber pressure, or adding PZ to the AMP solution. Increasing absorber pressure would require flue gas compression, thicker vessel walls, and additional plant supports, leading to higher design and operational costs, which is undesirable. Although PZ is known to be a promoter for the amine systems, its main disadvantage is the narrow operating loading range due to solubility limitation [32,33]. Therefore, increasing the surface area of packing is considered as the most suitable option, and the Mellapak 350Y packing was chosen for the scaled-up model because of the better capture efficiency [34]. The capture plant for the AMP solvent is scaled up to accommodate flue gas from an NGCC power plant [35]. The flue gas composition is presented in supplementary information (Table S3).

3.2. Procedure for scale-up

Scaling up is done using the methodology described by Kister [36] to achieve a capture level of 90%. The operational data for the scaled-up PCC plant are given in Table 6.

Table 6. Operating conditions for the full-scale AMP-based process model in Aspen Plus

Plant Specifications	Value
Absorber pressure (bar)	1.013
Flue gas inlet temperature (°C)	40
Lean loading (mol/mol)	0.20
Lean solvent concentration ($\%_{wt}$)	30.0
Packing type	Mellapak 350Y
CO_2 capture level	0.90
Reboiler temperature (°C)	120
Stripper pressure (bar)	1.65
Number of stages	20

Two criteria were used to determine the column diameter for given gas and liquid flow rates: the maximum pressure drop; and the approach to maximum capacity. A maximum pressure drop of 20.83 mm-H_2O/m is used [36,37], while the approach to maximum capacity ranges from 70-80% of the flooding point velocity for packed columns [36]. The capacity of

the column is characterised by its cross-sectional area and the column diameter confirmed from the generalised pressure drop correlation (Eq. 1):

$$D = \sqrt{\frac{4G}{\pi US}} \quad (1)$$

where G is the gas flow rate and U_s is the superficial velocity of the gas stream, which is associated with the packed column capacity factor by Eq. 2 [37,38].

$$C_o = U_s \left(\frac{\rho G}{\rho L - \rho G}\right)^{0.5} F_p^{0.5} {}_V{}^{0.05} \quad (2)$$

where C_o is the capacity factor; F_p is the packing factor; ρ_L and ρ_G are densities of liquid and gas, respectively; and ν is the kinematic viscosity of the liquid. The capacity factor for a packed column is dependent on the flow parameter (X) and the pressure drop per unit height of the packing (ΔP).

The flow parameter is given by Eq. 3 in which L is the liquid flowrate [37,38].

$$X = \frac{L}{G}\left(\frac{\rho G}{\rho L}\right)^{0.5} \quad (3)$$

Generalised pressure drop correlation (GPDC) charts were established for both random and structured packing [37,38]. Because of the turndown ratio limitations, packed column diameters should not exceed 15 m [34], and the cross-sectional areas for the absorber and stripper should meet the capacity requirements. Therefore, the minimum number of absorbers and strippers depends on the desired column capacity. These calculated estimates were used as an initial guess to scale up the model in Aspen Plus with the operating conditions set in order to prevent the column flooding to exceed 80%. Therefore, two absorption columns, each with a diameter of 15 m and one stripper with a diameter of 8.1 m are implemented into the model. The design and operations for the scaled-up AMP-based process are given in the supplementary information (Table S4).

4. Process analysis of capture plant

4.1. Sensitivity analysis

The reboiler duty accounts for most energy consumed in a post-combustion chemical absorption capture process and, therefore, it requires major consideration when comparing CO_2 solvents. The heat provided by the reboiler heats up the rich solvent from the absorber leading to the reverse of the CO_2 absorption reactions. CO_2 bonded in the form of carbamates

and bicarbonates is released, leaving the solvent behind, which is then recycled and reused in the absorber.

The reboiler duty can be reduced by optimising the lean solvent loading, the solvent concentration, and the stripper operating pressure. The scaled-up capture plant is used to study the effects of these key parameters in order to determine near-optimal operating conditions, and the key parameters are varied in the range:

- AMP solvent concentration, 25–35%$_{wt}$;
- Lean loading, 0.15–0.36 mol/mol;
- Stripper pressure, 1.5–3.5 bar.

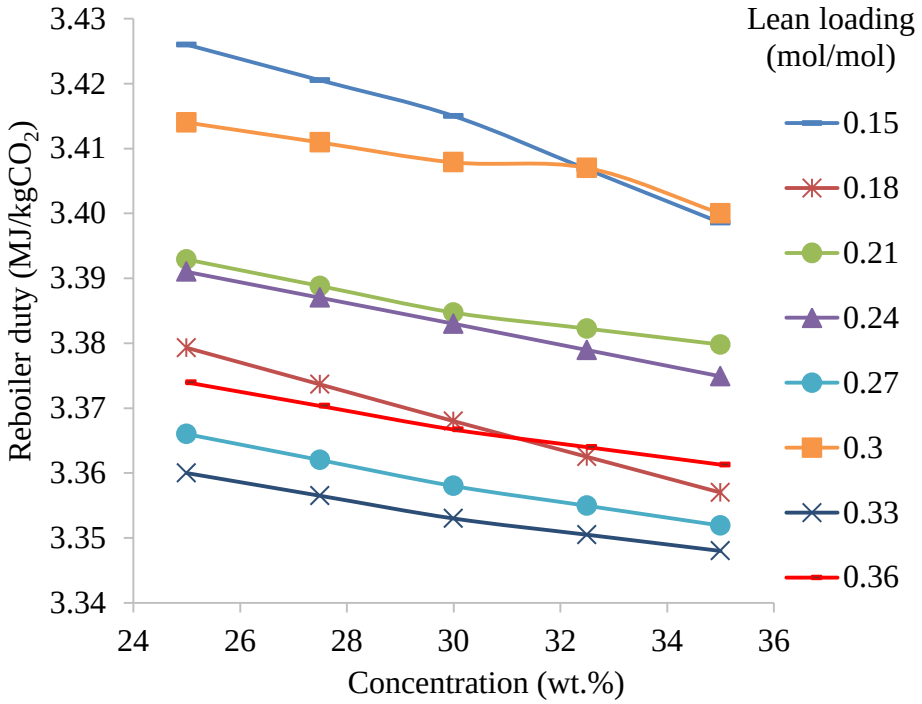

Fig. 3. Effect of solvent concentration and lean loading on reboiler duty

As shown in Fig. 3, an increase in solvent concentration results in a reduction in reboiler duty. This is driven mainly by the slightly reduced circulation rate as shown in Fig. 4, and because of the lower amount of water in the system, which means that less heat is needed to heat up and evaporate this water. Finally, it can be seen from Figs. 3 and 4 that minimum reboiler duty is achieved for 35%$_{wt}$ AMP and a lean loading of 0.33 mol/mol, and these values are selected to analyze the effect of stripper operating pressure.

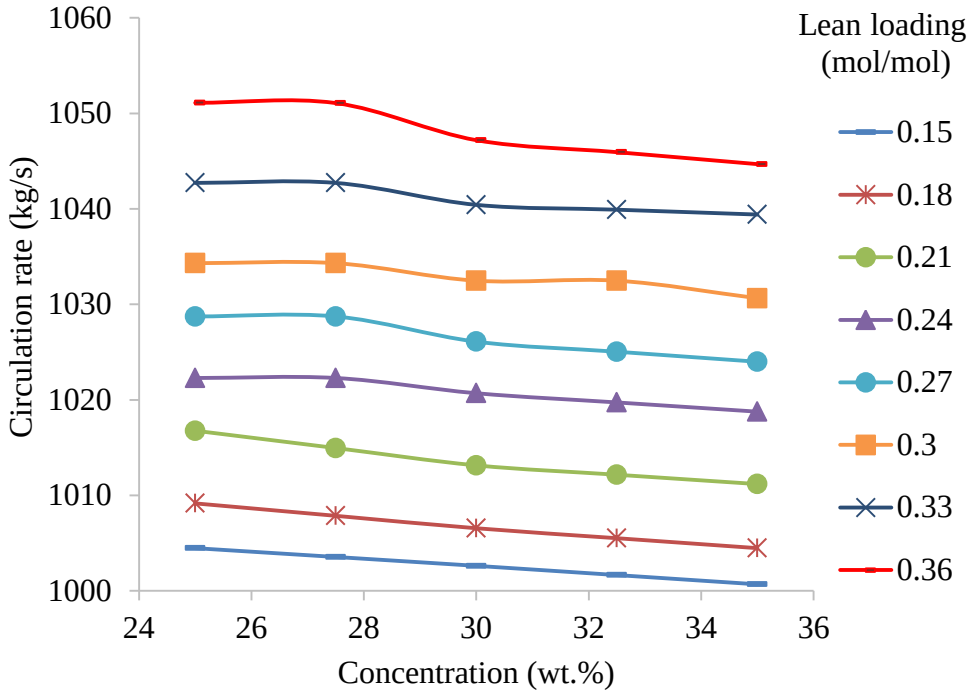

Fig. 4. Effect of solvent concentration on circulation rate

As shown in Fig. 5, with increasing stripper pressure, the reboiler duty temperature is higher while the reboiler duty decreases. For the range considered, the minimum reboiler duty is obtained at a stripper pressure of 3.5 bar and a reboiler temperature of 140°C. This is the highest recommended, which is limited by thermal degradation of AMP [14].

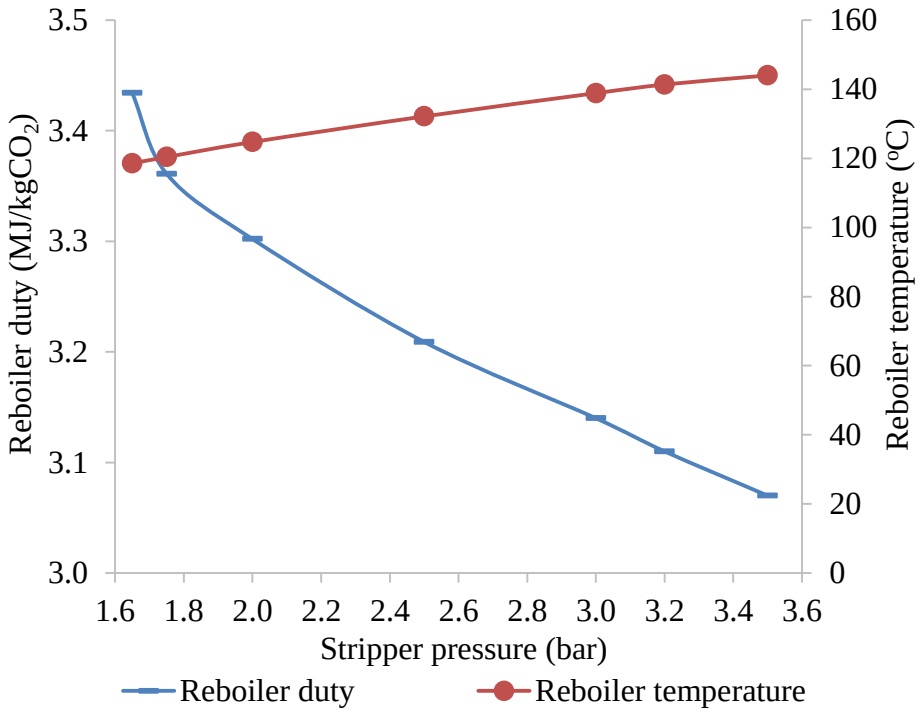

Fig. 5. Effect of stripper pressure on reboiler duty and reboiler temperature for AMP solvent

In order to have a benchmark for comparison, an MEA-based process model is scaled up using the same procedure described in Sections 3.1 and 3.2, with operational requirements given in the supplementary information (Table S5). The same flue gas composition and the plant specifications are used to design the MEA-based process.

5. NGCC power plant and compression train modelling

5.1. Power plant modelling

A 474 MW_e NGCC power plant with a net efficiency of 47.5%$_{LHV}$ is modeled in Aspen Plus® V8.4 and is used in this study to explore the performance of the NGCC retrofitted with the PCC. The NGCC plant comprises a single F-class gas turbine (GT), a heat recovery steam generator (HRSG), and a steam turbine. The GT is modelled based on the Peng-Robinson equation of state with a pressure ratio of 18.4. The Gibbs reactor was used to model the combustor [39]. The HRSG is configured with HP, IP, and LP steam drums, and superheater, reheater, and economiser sections, and the steam/water sides are modelled using the steam tables (STEAMBS). The HRSG recovers heat from the flue gas and produces steam for the steam cycle, that comprises the high-pressure (HP), intermediate-pressure (IP) and low-pressure (LP) turbine characterised by design isentropic efficiencies of 85%, 91.1%, and 92.7%, respectively [39].

Furthermore, the purpose of the feedwater system is to pump feed water streams from the deaerator storage tanks in the HRSG to the respective steam drums. The steam cycle condenser has a pressure of 0.07 bar, with an associated saturation temperature of 38.4°C. The boiler feed water pumps are driven by a boiler feed water turbine and extracted steam from the IP-LP crossover is expanded in the boiler feed water turbine. The steam needed by the CO_2 capture plant is also tapped from the IP-LP crossover while the condensate from the stripper reboiler is returned to the steam cycle deareator. The design parameters of the NGCC plant are provided in Table 7, and the model is validated with literature data [35]. The NGCC plant model predicts a net output of 448.3 MW_e with a net efficiency of 45.0%$_{LHV}$. A comparison of the stream data provided in the supplementary information (Tables S1 and S2) shows that the model is in close agreement with the literature data, and the majority of parameters have a deviation lower than 10%.

Table 7. NGCC design specifications

Parameter	Value
Fuel lower heat value $_{LHV}$ (MJ/kg)	47.45
Natural gas flow rate (kg/s)	21.1
Ambient air temperature (°C)	15
HP inlet pressure (bar)	166.5
IP inlet pressure (bar)	24.8
LP inlet pressure (bar)	5.2
Superheated steam temperature (°C)	565
Air to combustion ratio (wt.)	41.6
Turbine inlet temp (°C)	1273
Turbine inlet pressure (bar)	17.5
Condenser pressure (bar)	0.07
Thermal input $_{LHV}$ (MW_t)	997.0
Generator efficiency (%)	98.5

5.2. CO_2 compression train

There is an additional energy penalty incurred due to the requirement for the concentrated CO_2 compression in the CO_2 compression unit (CCU). Incorporation of this subsystem in the analysis helps to fully assess the performance of the retrofitted system. CO_2 leaves the desorber at 40°C and 3.5 bar and is then compressed to 110 bar in the compression section. The CO_2 compression unit comprises a multiple-stage centrifugal compressor with stage intercoolers, which help to reduce the operating temperatures of the compressor and knock-out drums, which reduce the power requirements by removing water from the CO_2 stream, reducing the volumetric flow rate through the compressor stages. Power consumption for this unit was estimated assuming polytropic efficiencies of 78–79% for all stages [40,41]. In order to achieve minimal compression work, a pressure ratio of 1.99 is used; thus, it is assumed that each stage operates at the same pressure ratio, and each stage pressure ratio should not be higher than 3 because of equipment limitations [42]. Preliminary design data are given in Table 8.

Table 8. Compression train design data

Description	Value
Number of compressors	5
Compressor efficiency range (%)	80
Intercooler temperature (°C)	33
Inlet pressure (bar)	3.5

6. Process integration

6.1. Integration of the AMP-based process into the power plant

Integration of the NGCC, AMP-based process and the CCU models is presented in this section. The flowsheet of the retrofitted system is shown in Fig. 6. The NGCC plant supplies steam for solvent regeneration, and electricity for the CCU and other auxiliary equipment. The PCC plant is integrated into the power plant at four points: (i) the flue gas stream from the power plant is fed into a single absorber in the PCC plant, (ii) the steam from the IP/LP crossover pipe is used to regenerate solvent in the reboiler, (iii) condensate is returned from the reboiler to the steam cycle, and (iv) the concentrated CO_2 stream from the regenerator is sent to the CO_2 compression train. A direct contact cooler (DCC) is used to cool down the flue gas coming from the power plant to 40°C before it is fed to the absorber. The IP/LP crossover is used to draw off steam from the steam cycle, which employs a throttle valve ensuring that the pressure across the IP/LP crossover does not fall below the value required in the reboiler, 3.5 bar. This steam supplied for regeneration needs to be at a minimum of 150°C so that the saturated solvent in the reboiler can be heated up to 140°C. In order to determine the pressure drop across the turbine sections, Stodola's ellipse, which is widely used for determination of the off-design performance in power plants [43], is used (Eq. 4).

$$\frac{m_1}{m_1^o} = \sqrt{\frac{T_1^o}{T_1}} \sqrt{\frac{p_1^2 - p_2^2}{p_1^{o\,2} - p_2^{o\,2}}} \tag{4}$$

where m_1, T_1, and p_1 are the inlet mass flowrate (kg/s), temperature (°C), and pressure (bar), respectively at off-design conditions, and m_1^o, T_1^o, and p_1^o are corresponding values at design conditions, while p_2 and p_2^o are the steam outlet pressures (bar) at off-design and design conditions, respectively.

6.2. Thermodynamic performance analysis

The process thermodynamic performance parameters of the retrofitted AMP-based process are presented in Table 9. In addition, for the purpose of comparison of the AMP-based process, the MEA-based process is also retrofitted and the key thermodynamic performance parameters are presented in Table 9. As discussed above, the reboiler duty can be considered as a key performance parameter in the retrofitted systems, which reflects benefits of the process employing AMP instead of MEA. The main differences in the operation of the AMP-based and MEA-based process retrofits are conditions in the stripper:

3.5 bar and 140°C, and 1.8 bar and 120°C respectively. Thus, this is enabled due to the better thermal stability of AMP. The pressure at the IP/LP crossover is 5.2 bar, i.e., more than required (4.8 bar, saturation temperature of 150°C) to reach 3.5 bar in the stripper, which proves process feasibility under the conditions considered for AMP. It can be seen in Table 9 that the integration of the AMP-based process results in 13.3% lower net power output (465.3 MWe *vs.* 536.8 MWe) compared to the reference NGCC. In addition, the net efficiency reduced from 53.8%$_{LHV}$ to 46.7%$_{LHV}$. Nevertheless, the thermodynamic performance of the AMP-based process with efficiency penalty of 7.1% points is superior to that of the MEA-based process, for which the efficiency penalty was estimated to be 9.1% points.

The Stodola's ellipse estimates that the pressure at the LP turbine inlet drops to 3.2 bar and 2.4 bar for AMP and MEA, respectively. Thus, the efficiencies for AMP and MEA without the effect of Stodola's ellipse are 47.3% and 45.6%, respectively, amounting to an additional 1% efficiency loss, compared to the retrofitted plant process when Stodola's ellipse is not taken into consideration; this is in accordance with the literature data [44,45] and indicates that the effects of changes in the pressure profile across the turbine sections need to be accounted for in assessing the PCC integration impact.

Table 9. Energy performance of the AMP-based and MEA-based process retrofits

Parameter	NGCC power plant without capture	Integration with MEA-based process	Integration with AMP-based process
Input parameters			
Stripper pressure (bar)		1.8	3.5
Stripper temperature (°C)		124	140
Output parameters			
Net power output (MWe)	536.8	445.9	465.3
Power loss (%)		16.9	13.3
Efficiency, LHV (%)	53.8	44.7	46.7
Efficiency penalty (%)	-	9.1	7.1
Power plant auxiliary load (kWe)	2636	2631	2707
Other auxiliary loads (kWe)[a]	6730	9840	9840
Net specific emissions ($kgCO_2$/MWh)	377.3	33.5	51.1
Steam draw-off flowrate (kg/s)	-	75.5	53.8
LP turbine pressure (bar)	5.2	2.4	3.2
CO_2 capture auxiliary load (MWe)	-	18.14	16.81
CO_2 compressor power (kWe)		2332	985
Reboiler duty (MJ/$kgCO_2$)	-	3.9	2.9
Required steam pressure (bar)	-	3.0	4.8

[a]Assumed based on the values of auxiliary loads reported in the US DOE report [35]

The CCU power requirement reduced from 2332 kW (MEA-based process, 1.8 bar) to 985 kW (AMP-based process, 3.5 bar), which leads to a parasitic load distribution of 2.7% for MEA and 1.5% for AMP as shown in Fig. 7 and Fig. 8, respectively. This is because the compressor train discharge pressure is fixed at 110 bar and, therefore, the higher suction pressure of 3.5 bar coming from the stripper results in reduced compression power required. Figs. 7 and 8 show the parasitic load distribution using the MEA solvent and the AMP solvent, revealing that the most important driver causing a reduction in net power output was the LP steam extraction for solvent regeneration; with a pressure of 3.5 bar (68.7%) for AMP and 1.8 bar (72.8%) for MEA. The electricity demand imposed on the power plant because of auxiliaries and the CCU integration contributes about 27.2% and 31.4% for MEA and AMP, respectively; this difference is due to the higher pumping duty for a pressure of 3.5 bar. As shown in Table 9, power output is higher for the AMP when compared to MEA. This, in turn, resulted in the less low-pressure steam generation and a drop in its pressure, which has been estimated according to the Stodola's ellipse; hence lower net power output is obtained for the MEA.

Also in Table 9, the results show a significant reduction in reboiler duty of the AMP process, 25.6%, compared to that of the MEA process. The main reason for this is the lower heat required for regeneration of AMP. It should also be noted here that the lower reboiler duty for AMP implies lower cooling duty, which results in additional benefits such as lower amounts of contaminated water to be treated and in general, smaller equipment and lower capital costs.

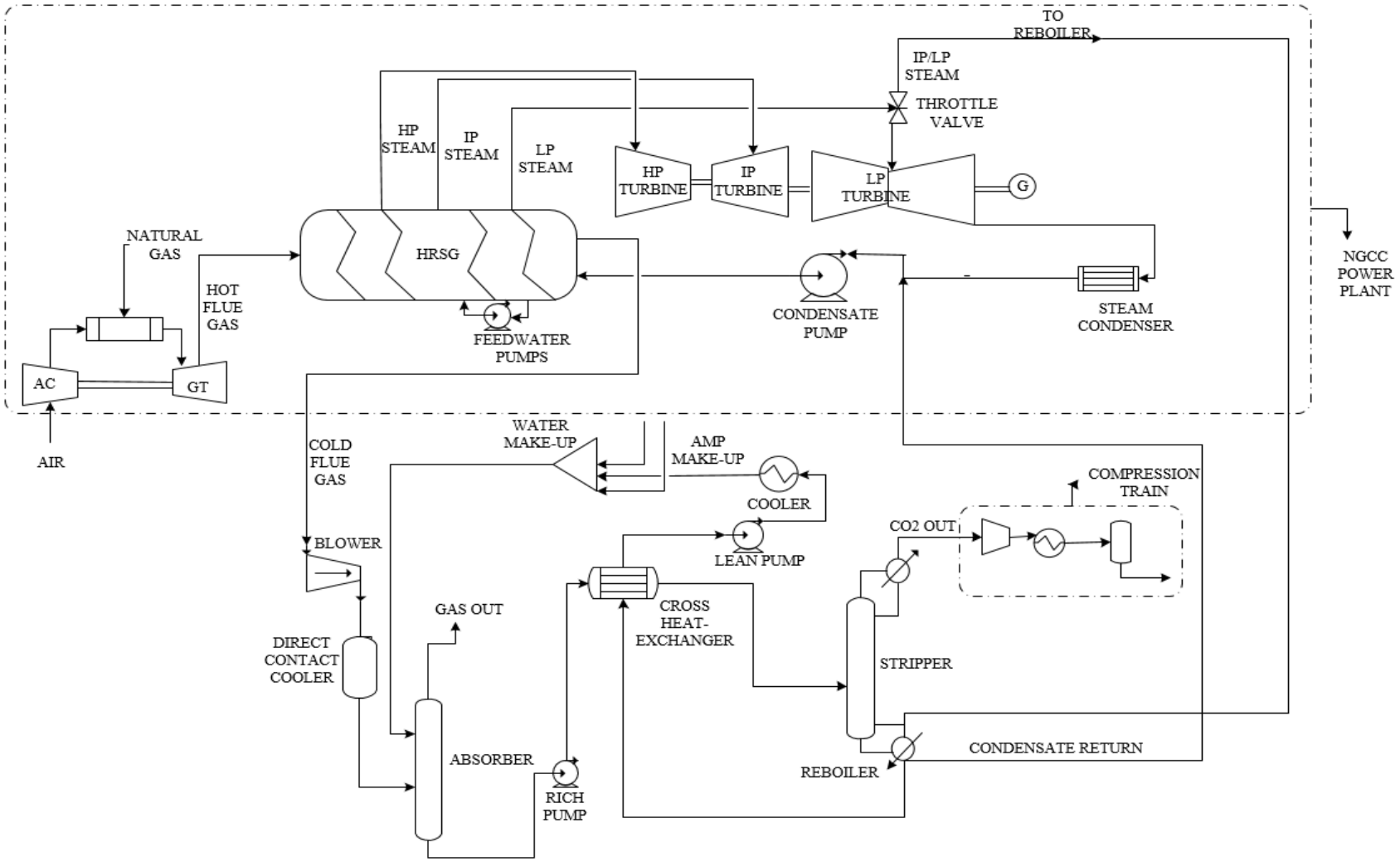

Fig. 6. Process flowsheet of the NGCC power plant retrofitted with AMP-based process and CO_2 compression unit

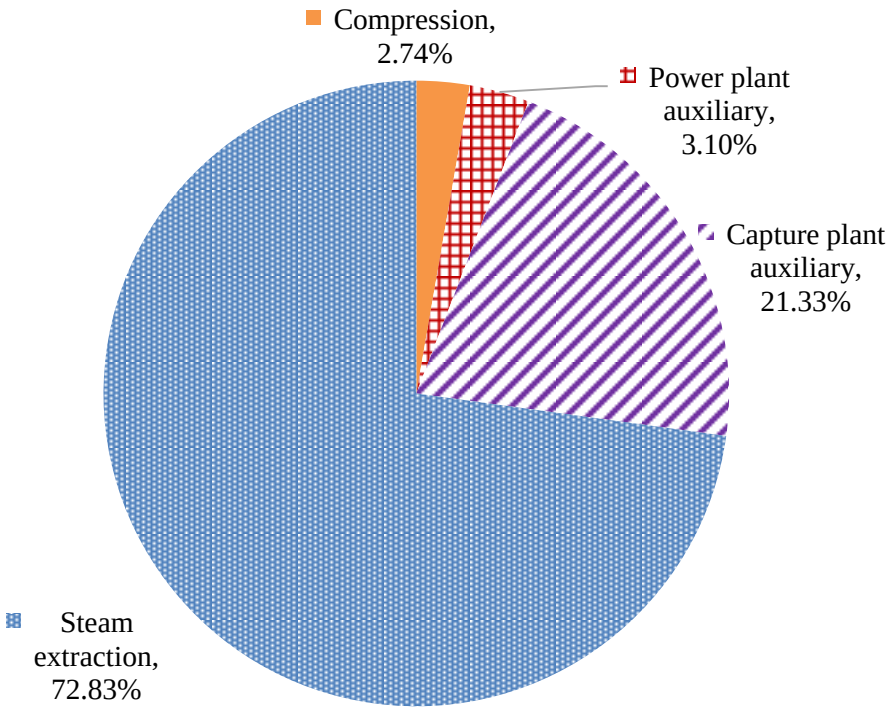

Fig. 7. Parasitic load distribution for NGCC retrofit with MEA-based process

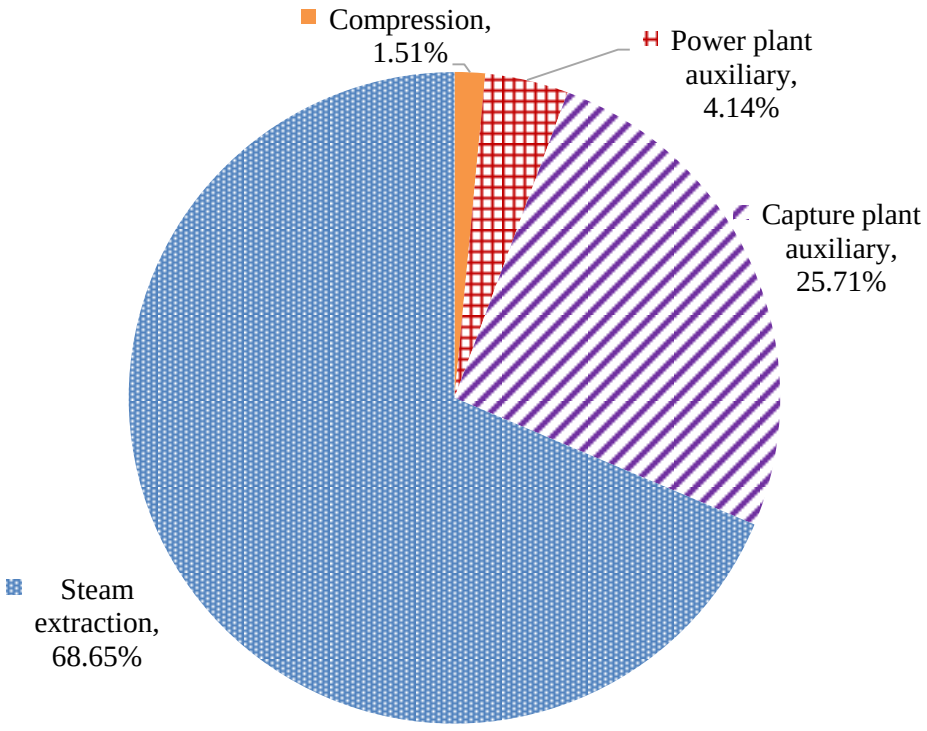

Fig. 8. Parasitic load distribution for NGCC retrofit with the AMP-based process

7. Economic analysis

7.1. Considerations

The estimation methodology employed for the capital cost, and the operating and maintenance cost (O&M) is discussed in this section. The cost figures (capital and O&M costs) for the NGCC power plant are obtained based on estimates from the DOE report [35]. The year of cost estimation in the literature data [35] is different from this study, therefore, the chemical engineering plant cost index [46], presented in Eq. 5 is used to escalate the prices to 2013 US dollars. The annual averaged CEPCI for the years; 2007, 2011 and 2013 are 525.4, 585.7 and 567.3, respectively [47].

$$\text{Present cost} = \text{original cost} \times \left\{\frac{CEPCI\ at\ present}{CEPCI\ at\ time\ original\ cost\ was\ obtained}\right\} \quad (5)$$

Aspen Process Economic Analyser® V8.4, which is based on the industry-standard Icarus System [48], is used in performing the economic analysis of the PCC plant with compression train. The bottom-up approach is used to generate the capital cost, which depends on material cost and wage rates, for estimation of equipment fabrication and cost of installation. The steps to obtain the capital and operating costs are described in Fig. 9.

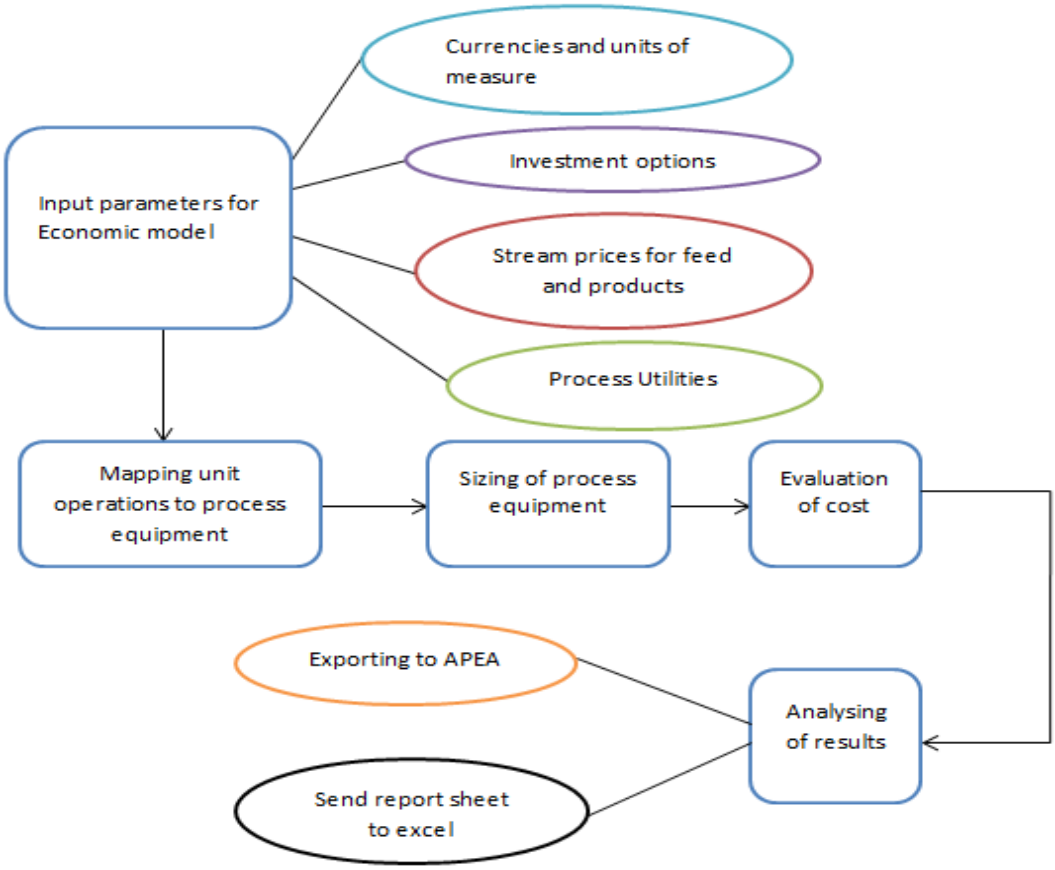

Fig. 9. Flowchart of economic analysis framework

The capital cost and the O&M cost of the capture plant with the compression train are calculated using the costing template for the USA, which uses 2013$ as the cost basis. Important cost inputs and assumptions are given in Table 10.

Table 10. Economic analysis assumptions and cost inputs

Input Parameters	Value
Plant location [35]	Greenfield, Midwestern USA
Plant capacity factor (%) [35]	85
Base year (year of capital expenditure)	2013
Operational period (year) [35]	30
Interest rate (%) [48]	10
Raw material escalation (%) [48]	3.5
Operating hours (h/year) [48]	8000
Natural gas price ($/GJ) [49]	3.94
AMP price (€/kg) [25]	8.0
MEA price (€/kg) [25]	1.0
Exchange rate (€/US$)	0.95

To assess the profitability of the proposed processes with respect to the reference NGCC, three cost metrics are evaluated for the reference NGCC and the retrofitted capture plants.

- Levelised cost of electricity accounts for the total lifetime unit cost of electricity of the plant [35]:

$$\mathrm{LCOE} = \frac{\mathrm{FCF\ X\ TOC + FOM + CF\ (VOM + FC)}}{\mathrm{CF\ X\ Wnet\ X\ 8760}} \quad (6)$$

Where $\mathrm{FCF} = \frac{\mathrm{i(1+i)^n}}{\mathrm{(1+i)^n - 1}}$

- CO_2 avoidance cost is given as:

$$\text{Cost of } \mathrm{CO_2 Avoided} = \frac{\mathrm{LCOE_{with\ capture}} - \mathrm{LCOE_{ref}}}{\text{tonne CO2 Emitted/(MW)}_{\mathrm{ref}} - \text{tonne CO2 Emitted/(MW)}_{\text{with capture}}} \quad (7)$$

- The cost of CO_2 captured is given as [50]:

$$\text{Cost of } \mathrm{CO_2} \text{ captured} = \frac{\mathrm{LCOE_{capture}} - \mathrm{LCOE_{ref}}}{(\mathrm{tCO2/MWh})_{\mathrm{captured}}} \quad (8)$$

where $(\mathrm{tCO_2/MWh})_{\mathrm{captured}}$ is the difference between the CO_2 produced and the CO_2 emitted.

To evaluate the economic viability of the retrofitted processes, these parameters: total overnight capital cost (TOC), fuel cost (FC), W_{net} (power output), fixed (FOM) and variable (VOM) operating costs and the fixed charge factor (FCF), which consider the total lifetime

cost and the interest rate of the project, are estimated. These economic estimates are presented in Table 11.

7.2. Economic performance assessment

The economic performance of the AMP and MEA-based processes retrofitted into the NGCC power plant is shown in Table 11. The O&M for the capture plant comprises fixed cost (maintenance, plant overhead, operating charges, and operating labour costs) and variable cost (solvent make-up cost and utility costs).

Table 11. Economic analysis for AMP-based and MEA-based processes

	NGCC power plant	Integration with MEA-based process	Integration with AMP-based process
Total overnight cost (M$)	430.1	781.1	762.7
Fuel cost (M$/a)	123.9	123.9	123.9
Fixed cost (M$/a)	13.2	40.0	39.5
Variable cost (M$/a)	5.9	20.0	16.0
Total O$M costs (M$/a)	142.1	183.9	179.3
LCOE ($/MWh)	42.7	74.8	69.9
CO_2 avoidance cost ($/t)		93.4	83.4
Cost of CO_2 captured ($/t)		78.4	69.3

The results of the different scenarios considered showed that the fuel cost dominates the O&M cost. The overnight capital cost for the NGCC power plant is 430.1 M$ which increased to 781.1 M$, and 762.7 M$ for the MEA and AMP, respectively, which is comparable with the data presented in the literature [26,35]. The operating cost for the MEA is 183.9 M$ and reduced to 179.3 M$ for that of the AMP. The better performance of the AMP-based process is mainly related to the reduced cost of compressors, while the operating cost is associated with the maintenance cost and the cost of utilities consumed, which includes the cost of steam, electricity, and cooling water.

The LCOE for the NGCC power plant is $42.7/t, which increased to $74.8/t and $69.9/t, for the MEA and the AMP, respectively. Thus, the LCOE for the NGCC power plant retrofit with the AMP-based process is 6.6% lower than that of the plant with the MEA. The CO_2 avoidance cost, which depends on the cost parameters and CO_2 emissions of the NGCC power plant, is estimated to be $93.4/t$CO_2$ and $83.4/t$CO_2$ for the retrofitted MEA and AMP-based processes, respectively. This aligns well with previous studies presented in the literature with a range of $35/t–$121/t for NGCC power plants [35,51]. In addition, the cost

of CO_2 captured with AMP reduced from \$78.4/t to \$69.9/t, which is 11.6% lower than that of MEA, and it is in range of the literature data (\$48/t–\$111.1/t) [51]. Therefore, the retrofitted process with the AMP solvent employing more favourable operating conditions appears to perform better than MEA-based process since it reduces the LCOE. The distribution of the cost is presented in Fig. 10.

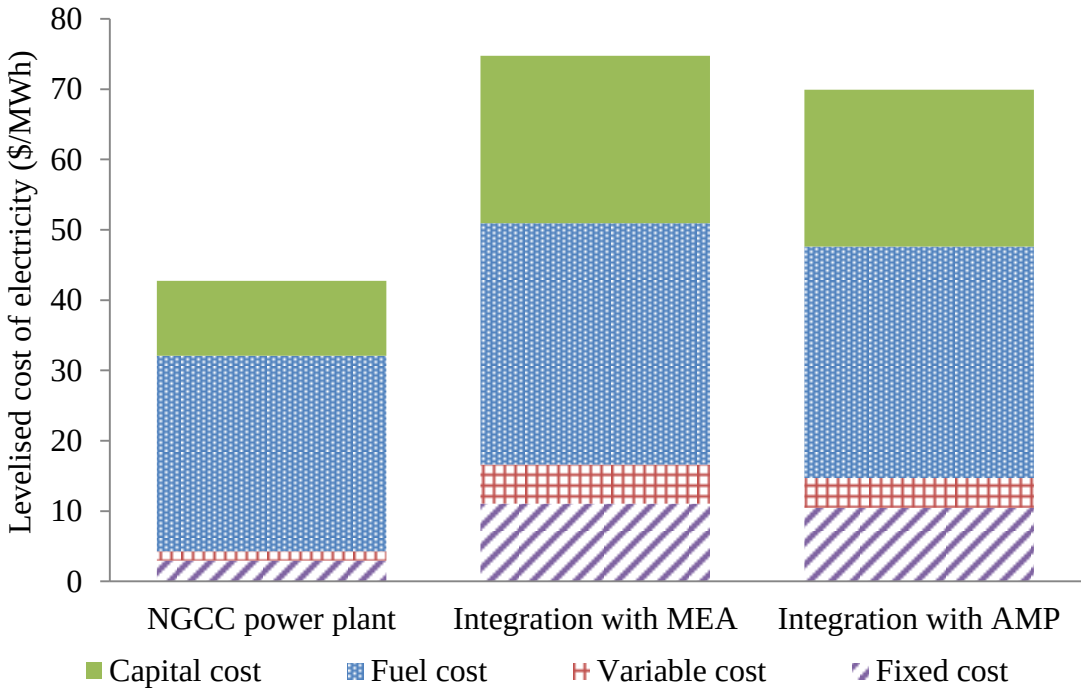

Fig. 10. Distribution of levelised cost of electricity by cost component

8. Sensitivity analysis

8.1.Variation of fuel cost

It has been recently shown that the cost of electricity is highly dependent on natural gas prices, and also for the NGCC power plants, the fuel cost is the dominating component of LCOE [35,52]. The sensitivity of LCOE to fuel cost is presented in Fig. 11. It can be seen that for a fuel price of \$6.55/MMBTU (\$6.9/GJ), LCOE is \$62.8/GJ, which is similar to LCOE values in studies using the same fuel cost [35]. On the other hand, it is observed that the AMP-based process has a lower LCOE compared to that of the MEA-based process. This is mainly due to the lower energy intensity of the former process, as shown in Table 10. In addition, at a low fuel cost of up to \$1.94/GJ, the increase in LCOE for MEA is 7.1% higher than that of AMP, while at a high fuel cost of up to \$9.94/GJ, the LCOE for MEA increases up to 5.6% higher than for AMP.

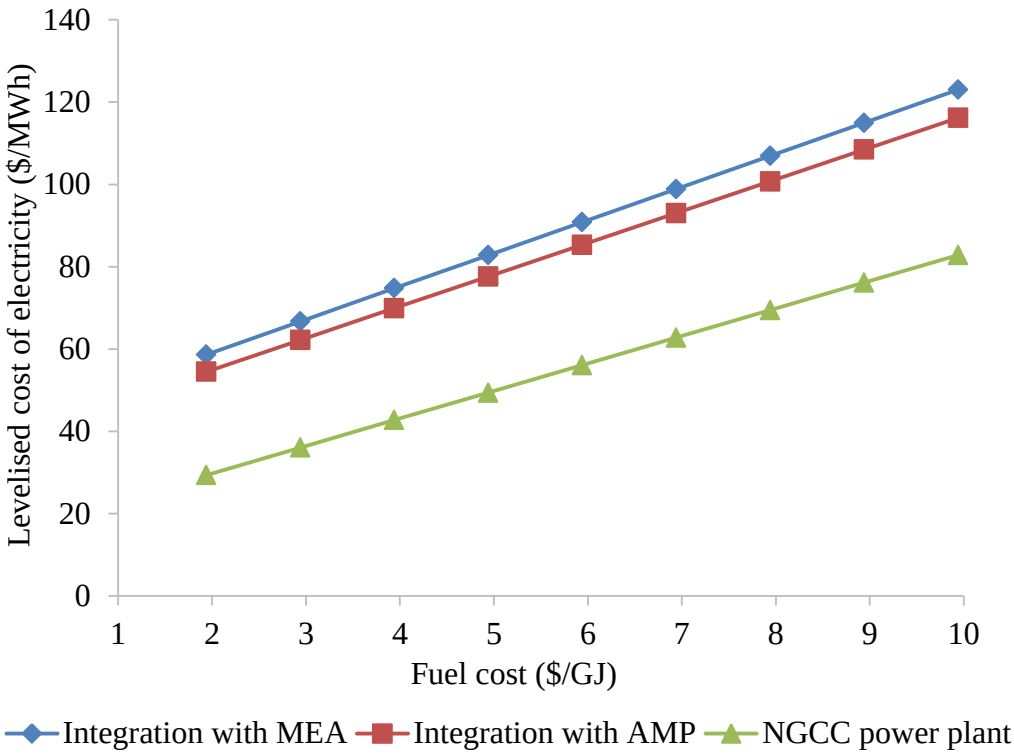

Fig. 11. Effect of fuel cost on levelised cost of electricity

8.2. Variation of capacity factor

The annual capacity factor (CF) of the NGCC is the ratio of its actual generation (that is, the unit's annual kWh) to the kWh it would generate if, hypothetically, it could operate at full capacity for every hour of the year without interruption. Most of the economic feasibility assessments in the previous studies [35] assumed that this factor is constant. However, as CF directly affects the LCOE, it is essential to assess the effect of its variation on the LCOE. Therefore, CF of the retrofitted system with the different solvents considered in this study is varied between 30% and 85%.

The results presented in Fig. 12 show that the LCOE decreases with increased CF. Due to the higher capital cost for the MEA-based process, the LCOE is higher by 6.3-7.0% than that of the AMP-based process across the considered CF range. In addition, the NGCC power plant will always be the most economical option in respect of the changes in the operational pattern of the system to meet the market demand. These results are important for decision makers in order to estimate the costing structure for an NGCC plant with PCC.

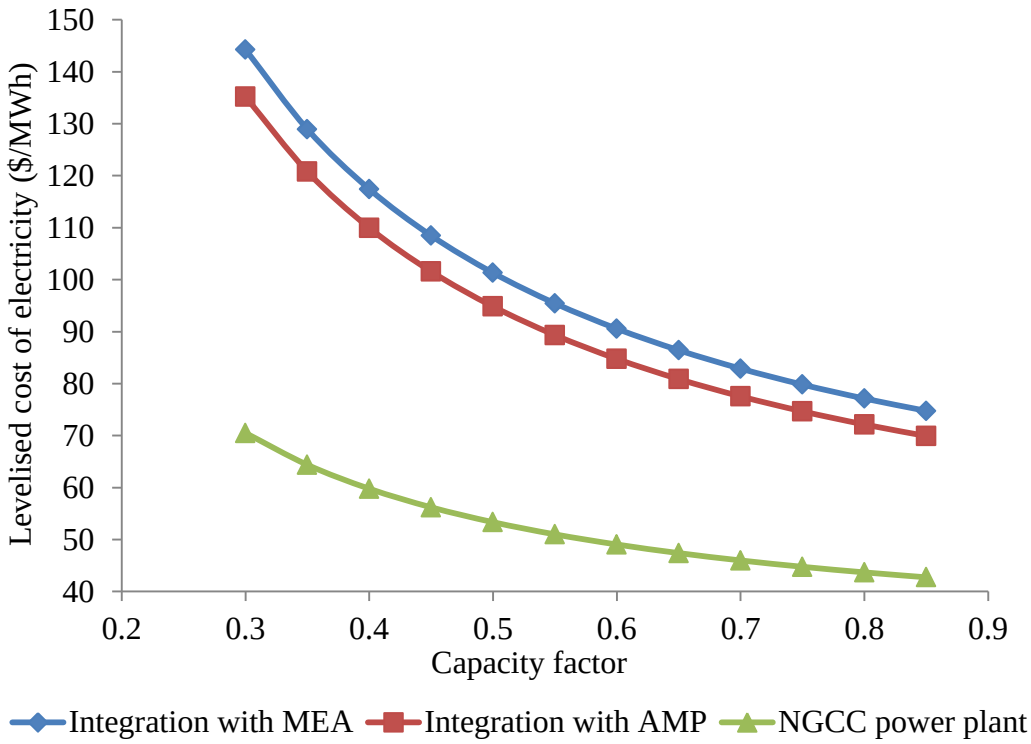

Fig. 12. Effect of capacity factor on levelised cost of electricity

8.3.Variation of make-up flowrate

The solvent make-up flowrate is a key parameter that affects the economics of the process plant. However, for the solvent-based processes, the loss of solvent frequently occurs as a result of its volatility, degradation, and fugitive emissions [53–55]. Therefore, feeding fresh solvent is needed in the system to make up for the losses. The case without makeup is presented in Section 7.2 (Table 11), while the solvent make-up rate is expressed as a percentage of total solvent flowrate in the PCC [56], as shown in Fig. 13. This aims to evaluate the effect of solvent make-up on the LCOE.

As shown in Fig. 13, the LCOE gradually increases with increase in the make-up flow rate. Results also show that when the makeup is taken into consideration, the LCOE for the AMP-based process becomes higher than that of the MEA-based process. This can be associated with the higher specific cost of AMP solvent, which is the major contributor to the variable cost. As shown in Table 10, the cost of AMP solvent is about eight times the cost of MEA solvent. In addition, AMP is known to be more volatile than MEA [54]. This implies that more solvent will be lost during the operation, and the AMP system will require a higher make-up rate. Also, Fig. 13 presents the sensitivity of LCOE to solvent price. The cost of

solvent for both AMP and MEA is varied by ±25%, and the results show that the LCOE in the AMP case is more sensitive to price changes, which is expected due to the higher price of AMP. Importantly, such results imply that although the use of AMP as a solvent in chemical solvent scrubbing can significantly reduce the efficiency penalty associated with CO_2 capture from NGCCs, it may not be the most economically-feasible option if the make-up rate is above 0.03%. Thus, this make-up rate of 0.03% is below the expected value for amine scrubbing [56]. It needs to be stressed, therefore, that development of novel CO_2 capture materials needs to be substantiated from both thermodynamic and economic standpoints.

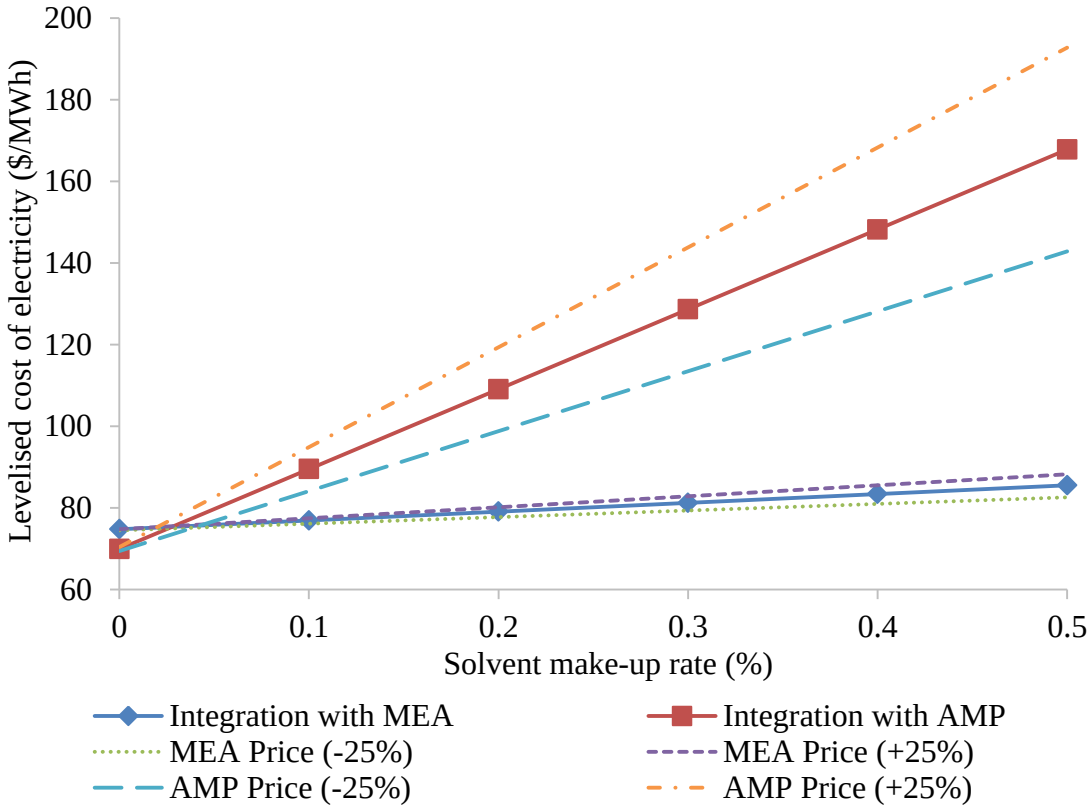

Fig.13. Effect of make-up rate on levelised cost of electricity

9. Conclusions

In this study, a post-combustion capture process with AMP solvent is evaluated. AMP is considered to potentially replace traditional MEA solvent in the CO_2 capture processes. A detailed rate-based model implemented in Aspen Plus® was used to evaluate the PCC process. The model was developed in Aspen Plus® V8.4 at the pilot scale and validated using the experimental pilot plant data available in the literature [13]. The simulation results indicated good agreement between the pilot plant logs and the model predictions, especially

when the Billet and Schultes and Bravo and Rocha mass transfer correlations [28,30] were implemented in the absorber and stripper models, respectively. The model was then scaled up to process flue gas from a 400 MWe NGCC power plant. The effects of lean loadings, solvent concentration, and stripper pressure on reboiler duty were investigated. The simulations pinpointed the region for near-optimal operating conditions, which resulted in the lowest reboiler duty: AMP concentration of $35\%_{wt}$ with a stripper pressure and temperature of 3.5 bar and 140°C, respectively. These conditions resulted in 25.6% reduction in the reboiler heat duty required for solvent regeneration compared to that of the MEA-based process. In order to assess the impact of integration, the effect of steam extraction on the pressure profile was considered using Stodola's ellipse. The results proved that AMP solvent is of superior performance from the thermodynamic point of view, as it can reduce the efficiency penalties associated with the MEA-based process retrofits.

Economic analysis was performed for the retrofitted AMP- and MEA-based processes, using a bottom-up approach. The LCOE for the AMP-based process was found to be 6.6% lower than that of the MEA if no solvent make-up was considered. However, the LCOE becomes equal for both solvents if the make-up is only 0.03%. Beyond this point, the MEA-based process becomes more economically feasible, regardless of higher efficiency penalties. This implies that although the use of AMP as a solvent in chemical solvent scrubbing can significantly reduce the efficiency penalty associated with CO_2 capture from NGCCs, it may not be the most feasible option from the economic point of view. Therefore, evaluation of novel CO_2 capture materials should consider both thermodynamic and economic performance.

References

[1] IEA - International Energy Agency, Technology Roadmap, (2013). doi:10.1007/SpringerReference_7300.

[2] E.S. Rubin, C. Chen, A.B. Rao, Cost and performance of fossil fuel power plants with CO_2 capture and storage, Energy Policy. 35 (2007) 4444–4454. doi:10.1016/j.enpol.2007.03.009.

[3] A.B. Rao, Details of A Technical, Economic and Environmental Assessment of Amine-based CO_2 Capture Technology for Power Plant Greenhouse Gas Control. Appendix to Annual Technical Progress Report. Reporting period October 2000 - October 2001., (2002) 40.

[4] A.L. Kohl, R.B. Nielsen, Gas Purification, 1997. doi:10.1016/B978-088415220-0/50009-4.

[5] M. Lucquiaud, J. Gibbins, On the integration of CO_2 capture with coal-fired power plants: A methodology to assess and optimise solvent-based post-combustion capture systems, Chem. Eng. Res. Des. 89 (2011) 1553–1571. doi:10.1016/j.cherd.2011.03.003.

[6] S.T. Kim, J.W. Kang, J.S. Lee, B.M. Min, Analysis of the heat of reaction and regeneration in the alkanolamine-CO_2 system, Korean J. Chem. Eng. 28 (2011) 2275–2281. doi:10.1007/s11814-011-0126-1.

[7] S. Freguia, Modeling of CO_2 removal from flue gases with monoethanolamine, 2003. http://www.che.utexas.edu/rochelle_group/Pubs/FreguiaPubThesis.pdf.

[8] P. Galindo, A. Schäffer, K. Brechtel, S. Unterberger, G. Scheffknecht, Experimental research on the performance of CO_2-loaded solutions of MEA and DEA at regeneration conditions, Fuel. 101 (2012) 2–8. doi:10.1016/j.fuel.2011.02.005.

[9] N. MacDowell, N. Florin, A. Buchard, J. Hallett, A. Galindo, G. Jackson, C.S. Adjiman, C.K. Williams, N. Shah, P. Fennell, An overview of CO_2 capture technologies, Energy Environ. Sci. 3 (2010) 1645. doi:10.1039/c004106h.

[10] G. Sartori, W.S. Ho, D.W. Savage, G.R. Chludzinski, S. Wlechert, Sterically-Hindered Amines for Acid-Gas Absorption, Sep. Purif. Rev. 16 (1987) 171–200. doi:10.1080/03602548708058543.

[11] U.E. Aronu, H.F. Svendsen, K.A. Hoff, O. Juliussen, Solvent selection for carbon dioxide absorption, Energy Procedia. 1 (2009) 1051–1057. doi:10.1016/j.egypro.2009.01.139.

[12] P. Zhang, Y. Shi, J. Wei, W. Zhao, Q. Ye, Regeneration of 2-amino-2-methyl-1-propanol used for carbon dioxide absorption, J. Environ. Sci. 20 (2008) 39–44. doi:10.1016/S1001-0742(08)60005-4.

[13] J. Gabrielsen, H.F. Svendsen, M.L. Michelsen, E.H. Stenby, G.M. Kontogeorgis, Experimental validation of a rate-based model for CO_2 capture using an AMP solution, Chem. Eng. Sci. 62 (2007) 2397–2413. doi:10.1016/j.ces.2007.01.034.

[14] T. Wang, K.J. Jens, Oxidative degradation of aqueous 2-amino-2-methyl-1-propanol solvent for postcombustion CO_2 capture, Ind. Eng. Chem. Res. 51 (2012) 6529–6536. doi:10.1021/ie300346j.

[15] M.R.M. Abu-Zahra, Z. Abbas, P. Singh, P. Feron, Carbon Dioxide Post-Combustion Capture : Solvent Technologies Overview, Status and Future Directions, Mater. Process. Energy Commun. Curr. Res. Technol. Dev. (2013) 923–934.

[16] A. Aroonwilas, A. Veawab, Characterization and Comparison of the CO_2 Absorption Column, Ind. Eng. Chem. Res. 43 (2004) 2228–2237. doi:10.1021/ie0306067.

[17] F.A. Chowdhury, H. Okabe, H. Yamada, M. Onoda, Y. Fujioka, Synthesis, and selection of hindered new amine absorbents for CO_2 capture, Energy Procedia. 4 (2011) 201–208. doi:10.1016/j.egypro.2011.01.042.

[18] H.M. Kvamsdal, G. Haugen, H.F. Svendsen, A. Tobiesen, H. Mangalapally, A. Hartono, T. Mejdell, Modelling and simulation of the Esbjerg pilot plant using the Cesar 1 solvent, Energy Procedia. 4 (2011) 1644–1651. doi:10.1016/j.egypro.2011.02.036.

[19] S.K. Dash, A.N. Samanta, S.S. Bandyopadhyay, Simulation and parametric study of

the post-combustion CO_2 capture process using (AMP+PZ) blended solvent, Int. J. Green. Gas Control. 21 (2014) 130–139. doi:10.1016/j.ijggc.2013.12.003.

[20] A. Aboudheir, P. Tontiwachwuthikul, R. Idem, Rigorous model for predicting the behavior of CO_2 absorption into AMP in packed-bed absorption columns, Ind. Eng. Chem. Res. 45 (2006) 2553–2557. doi:10.1021/ie050570d.

[21] M. Afkhamipour, M. Mofarahi, Comparison of rate-based and equilibrium-stage models of a packed column for post-combustion CO_2 capture using 2-amino-2-methyl-1-propanol (AMP) solution, Int. J. Green. Gas Control. 15 (2013) 186–199. doi:10.1016/j.ijggc.2013.02.022.

[22] E. Osagie, C. Biliyok, G. Di Lorenzo, V. Manovic, Process modelling and simulation of degradation of 2-amino-2-methyl-1-propanol (AMP) capture plant, Energi Procedia 114 (2017) 1930–1939. doi:10.1016/j.egypro.2017.03.1324.

[23] M. Van der Spek, R. Arendsen, A. Ramirez, A. Faaij, Model development and process simulation of post-combustion carbon capture technology with aqueous AMP/PZ solvent, Int. J. Green. Gas Control. 47 (2016) 176–199.

[24] E. Sanchez Fernandez, E.L. V Goetheer, G. Manzolini, E. Macchi, S. Rezvani, T.J.H. Vlugt, Thermodynamic assessment of amine-based CO_2 capture technologies in power plants based on European Benchmarking Task Force methodology, Fuel. 129 (2014) 318–329. doi:10.1016/j.fuel.2014.03.042.

[25] G. Manzolini, E.S. Fernandez, S. Rezvani, E. Macchi, E.L. V Goetheer, T.J.H. Vlugt, Economic assessment of novel amine-based CO_2 capture technologies integrated into power plants based on European Benchmarking Task Force methodology, Appl. Energy. 138 (2015) 546–558. doi:10.1016/j.apenergy.2014.04.066.

[26] C. Biliyok, H. Yeung, International Journal of Greenhouse Gas Control Evaluation of natural gas combined cycle power plant for post-combustion CO_2 capture integration, Int. J. Greenh. Gas Control. 19 (2013) 396–405. doi:10.1016/j.ijggc.2013.10.003.

[27] I.. Aspen Technology, Rate-Based Model of the CO_2 Capture Process by AMP using Aspen Plus, Cambridge, MA, USA, 2008.

[28] P.D.-I.R. Billet, D.-I.M. Schultes, Predicting mass transfer in packed columns, Chem. Eng. Technol. 16 (1993) 1–9.

[29] F.J. Bravo JL, Rocha JA, Mass transfer in gauze packings. Hydrocarbon Processing., (1985) 64(1):91-5.

[30] J.R.F. Bravo, Jose L., J. Antonio Rocha, "A comprehensive model for the performance of columns containing structured packings." Institution of Chemical Engineers Symposium Series. Vol. 128. Hemisphere Publishing Corp., (1992).

[31] H.M. Kvamsdal, G.T. Rochelle, Effects of the temperature bulge in CO_2 absorption from flue gas by aqueous monoethanolamine, Ind. Eng. Chem. Res. 47 (2008) 867–875. doi:10.1021/ie061651s.

[32] S.A. Freeman, R. Dugas, D.H. Van Wagener, T. Nguyen, G.T. Rochelle, Carbon dioxide capture with concentrated, aqueous piperazine, Int. J. Greenh. Gas Control. 4 (2010) 119–124. doi:10.1016/j.ijggc.2009.10.008.

[33] L. Li, A.K. Voice, H. Li, O. Namjoshi, T. Nguyen, Y. Du, G.T. Rochelle, Amine blends using concentrated piperazine, Energy Procedia. 37 (2013) 353–369.

doi:10.1016/j.egypro.2013.05.121.

[34] Chemtech - Sulzer Chemtech, "Structured packings for distillation, absorption and reactive distillation." Sulzer Chemtech Ltd, Winterthur, (2010).

[35] NETL, Cost and Performance Baseline for Fossil Energy Power Plants study, Volume 1: Butiminous Coal and Natural Gas to Electricity, (2010).

[36] H. Kister, "Distillation DesignMcGraw-Hill.," (1992). New York

[37] R.F. Strigle, Packed tower design and applications: random and structured packings, (1994) 354.

[38] R.H. Perry, D.W. Green, Chemical Engineers' Handbook, (2008). New York

[39] NETL, Process Modeling Design Parameters, (2012).

[40] I. Pfaff, J. Oexmann, a. Kather, Optimised integration of post-combustion CO_2 capture process in greenfield power plants, Energy. 35 (2010) 4030–4041. doi:10.1016/j.energy.2010.06.004.

[41] S. Posch, M. Haider, Optimization of CO_2 compression and purification units (CO_2CPU) for CCS power plants, Fuel. 101 (2012) 254–263. doi:10.1016/j.fuel.2011.07.039.

[42] A.A. Ardiyansyah S, Md. Nor M, Wan A, Optimum number of stages of the new multi-stage symmetrical wobble plate compressor, Faculty of Mechanical Engineering Universiti Teknologi Malaysia, Skudai, Johor, Malaysia, (2006).

[43] D.H. Cooke, On Prediction of Off-Design Multistage Turbine Pressures by Stodola's Ellipse, J. Eng. Gas Turbines Power. 107 (1985) 596. doi:10.1115/1.3239778.

[44] C. Biliyok, R. Canepa, D.P. Hanak, Investigation of Alternative Strategies for Integrating Post-combustion CO_2 Capture to a Natural Gas Combined Cycle Power Plant, Energy & Fuels. 29 (2015) 4624–4633. doi:10.1021/acs.energyfuels.5b00811.

[45] D.P. Hanak, C. Biliyok, V. Manovic, Evaluation and modeling of part-load performance of coal-fired power plant with postcombustion CO_2 capture, Energy and Fuels. 29 (2015) 3833–3844. doi:10.1021/acs.energyfuels.5b00591.

[46] M.S. Peters, K.D. Timmerhaus, R.E. West, Materials Transfer, Handling, and Treatment Equipment-Design and Costs, 2004.

[47] Chemical Engineering, Economic Indicators, Chem. Eng. (2015) 64.

[48] I. AspenTech, Aspen Process Economic Analyzer V7.2 User Guide, Burlington, MA, USA, 2010.

[49] U.S. Energy Information Administration, Table 3, 2012.

[50] G.P. Hammond, S.S.O. Akwe, S. Williams, Techno-economic appraisal of fossil-fuelled power generation systems with carbon dioxide capture and storage, Energy. 36 (2011) 975–984. doi:10.1016/j.energy.2010.12.012.

[51] H.J.H. Edward S. Rubin, John E. Davison, The cost of CO_2 capture and storage, Int. J. Greenh. Gas Control. 40 (2015) 167–187. doi:10.1016/j.ijggc.2015.05.028.

[52] G. Di Lorenzo, P. Barbera, G. Ruggieri, J. Witton, P. Pilidis, D. Probert, Pre-combustion carboncapture technologies for power generation: an engineering-economic assessment, Int. J. Energy Res. (2013) 389–402.

[53] F. Vega, A. Sanna, B. Navarrete, M.M. Maroto-Valer, V.J. Cortes, Degradation of amine-based solvents in CO_2 capture process by chemical absorption, Greenh. Gases Sci. Technol. 4 (2014) 707–733. doi:10.1002/ghg.1446.

[54] T. Nguyen, M. Hilliard, G.T. Rochelle, Amine volatility in CO_2 capture, Int. J. Greenh. Gas Control. 4 (2010) 707–715. doi:10.1016/j.ijggc.2010.06.003.

[55] G.T. Rochelle, Amine scrubbing for CO_2 capture., Science. 325 (2009) 1652–1654. doi:10.1126/science.1176731.

[56] A. Cormos, C. Cormos, Techno-economic evaluations of post-combustion CO_2 capture from sub- and super-critical circulated fluidised bed combustion (CFBC) power plants, Appl. Therm. Eng. 127 (2017) 106–115. doi:10.1016/j.applthermaleng.2017.08.009.